Zeitschrift: Helvetica Physica Acta
Band: 53 (1980)
Heft: 3

Artikel: Quarkonium spectra in the framework of quantum chromodynamics
Autor: Viollier, R.D. / Rafelski, J.
DOI: https://doi.org/10.5169/seals-115122

Helvetica Physica Acta, Vol. 53 (1980), Birkhäuser Verlag, Basel

Quarkonium spectra in the framework of quantum chromodynamics[1])

by **R. D. Viollier**[2])

Center for Theoretical Physics, Laboratory for Nuclear Science and Department of Physics, Massachusetts Institute of Technology, Cambridge, Massachusetts 02139

and **J. Rafelski**[3])

CERN, Geneva, Switzerland

(10. VI. 1980)

Abstract. We study the nonrelativistic bound states of heavy quark-antiquark pairs in the framework of quantum chromodynamics. Our static potential is related to the Fourier transform of the 'dressed' gluon propagator. Aside from the quark masses, the model contains two free parameters:

(i) the scale parameter of the theory Λ, and

(ii) the radius r_0 where an additional confining force must be considered.

We evaluate the spectra of heavy quarkonium states solving the Schrödinger equation with our flavor independent potential. The spin dependent parts of the interaction are treated in first order perturbation based on the generalized Breit-Fermi interaction. We evaluate the leptonic decay widths and electromagnetic transition rates using spin independent wave functions.

With $\Lambda = 0.44$ GeV, $r_0 = 0.38$ fm, $m_c = 1.525$ GeV, and $m_b = 4.929$ GeV the charmonium and bottomium spectroscopy is reproduced very well. This can be interpreted as evidence for the validity of quantum chromodynamics. We also discuss the $(b\bar{c})$-spectrum and toponium spectrum as a function of the top quark mass m_t.

1. Introduction

It is now well accepted that the 'new resonances', e.g. J/ψ and Υ, are bound states of heavy quark-antiquark $(Q\bar{Q})$ pairs. The richness and form of the spectra suggest a description in terms of the Schrödinger equation [1] with a convex potential. Two families of such states, the $J/\psi \equiv (c\bar{c})$ and the $\Upsilon \equiv (b\bar{b})$ resonances, are known today. There is a strong theoretical expectation that at least one more family, $\zeta \equiv (t\bar{t})$, may exist which has a new type of heavy quark, the top quark t [2], as the fundamental building block.

The spectroscopic properties of these heavy quarkonium states represent a sensitive test for quantum chromodynamics (QCD) [3], the nonabelian gauge theory of strong interactions. The reason for this fact is that the nonrelativistic heavy quarks (c, b, t) essentially probe the static quark-antiquark potential. Many

[1]) This work is supported in part through funds provided by the U.S. Department of Energy (DOE) under contract EY-76-C-02-3069.

[2]) Present address: Inst. for Theoretical Physics, University of Basel, Switzerland.

[3]) Present address: Institute for Theoretical Physics, University of Frankfurt, West Germany.

studies of the charmonium ($c\bar{c}$) and bottomium ($b\bar{b}$) systems have been based on the Coulomb+linear potential for the static quark-antiquark interaction. This approach, motivated to some extent by QCD, has been fairly successful in the description of the charmonium spectrum [4, 5]. However, there are important vacuum polarization corrections [6–11] which will affect this simple form of the potential. The strong polarizability of the perturbative vacuum is reflected in the well-known property of asymptotic freedom [12], arising from the dependence of the running coupling 'constant' on the momentum transfer q,

$$\alpha(q^2)=\frac{1}{B_{Nf}\log(-q^2/\Lambda^2)}. \tag{1}$$

For a general $SU(N)_{\text{color}}\otimes SU(f)_{\text{flavor}}$ theory of strong interactions B_{Nf} is given by

$$B_{Nf}=(11N-2f)/12\pi \tag{2}$$

where N represents the number of colors, and f stands for the number of (massless) quark flavors contributing to the polarizability of the vacuum. From scaling violations in deep inelastic reactions [13], the scale Λ in equation (1) is expected to be within the range of $100\,\text{MeV}\lesssim\Lambda\lesssim 700\,\text{MeV}$.

Our intention is to show that the currently available quarkonium spectra lend a strong support towards QCD as the theory of interacting quarks. The spin independent static potential $W_0(r)$ is the Fourier transform of the Coulomb propagator dressed with the running coupling constant (1). For a general $SU(N)_{\text{color}}\otimes SU(f)_{\text{flavor}}$ theory we have

$$W_0(r)=-\frac{C_N}{2\pi^2}\int\frac{\alpha(-|\mathbf{q}|^2)}{|\mathbf{q}|^2}\,e^{-i\mathbf{qr}}\,d^3\mathbf{q} \tag{3}$$

where

$$C_N=(N^2-1)/2N \tag{3'}$$

is the color factor [14] of a $Q\bar{Q}$ system in a color singlet state. As compared to previous models [4–11], our approach will mainly improve the intermediate range behavior ($0.1\,\text{fm}\lesssim r\lesssim 0.4\,\text{fm}$) of the interaction. Since the potential (3) does not have the desired long-range property ($r\gtrsim 0.4\,\text{fm}$), we will assume that the confining part grows linearly beyond a certain radius r_0. The proper understanding of this sector is related to the confinement puzzle which will not be further discussed in this paper.

We describe the nonrelativistic system in terms of the Schrödinger equation ($\hbar=c=1$)

$$\left(-\frac{1}{m_Q}\boldsymbol{\nabla}^2+W\right)\psi=E\psi. \tag{4}$$

The total mass M of the bound state ψ is given by the quark mass M_Q and the binding energy $(-E)$, i.e.

$$M=2m_Q+E. \tag{5}$$

The spin structure of the interaction $W(\mathbf{r})$ has the general form [14]

$$W(\mathbf{r})=W_0(r)+W_1(r)\mathbf{L}\cdot\mathbf{S}+W_2(r)S_{12}+W_3(r)\boldsymbol{\sigma}_1\cdot\boldsymbol{\sigma}_2 \tag{6}$$

where **L** is the orbital angular momentum, S_{12} denotes the tensor operator

$$S_{12} = 3(\boldsymbol{\sigma}_1 \cdot \hat{\mathbf{r}})(\boldsymbol{\sigma}_2 \cdot \hat{\mathbf{r}}) - \boldsymbol{\sigma}_1 \cdot \boldsymbol{\sigma}_2 \tag{7}$$

and

$$\mathbf{S} = \tfrac{1}{2}(\boldsymbol{\sigma}_1 + \boldsymbol{\sigma}_2) \tag{8}$$

represents the total spin of the quark-antiquark pair.

The details of the spin independent potential $W_0(r)$ are determined by QCD, and will be given in Section 2. If $W_0(r)$ can be represented as a sum of a Lorentz vector and scalar piece

$$W_0(r) = V_0(r) + S_0(r) \tag{9}$$

the spin dependent potentials are found via the nonrelativistic reduction yielding the generalized Breit-Fermi interaction [14]

$$\begin{cases} W_1(r) = \dfrac{1}{2m_Q^2}\left(\dfrac{3}{r}\dfrac{dV_0}{dr} - \dfrac{1}{r}\dfrac{dS_0}{dr}\right), \\ W_2(r) = \dfrac{1}{12m_Q^2}\left(\dfrac{1}{r}\dfrac{dV_0}{dr} - \dfrac{d^2V_0}{dr^2}\right) \\ W_3(r) = \dfrac{1}{6m_Q^2}\boldsymbol{\nabla}^2 V_0. \end{cases} \tag{10}$$

In Section 3, we will solve the Schrödinger equation for heavy quark-antiquark systems. The spin dependent parts of the interaction are treated in first order perturbation theory. We compare the calculated $(c\bar{c})$ and $(b\bar{b})$ levels with the experimental data, and predict the $(t\bar{t})$ and $(b\bar{c})$ spectra. The leptonic decay widths and electromagnetic transition rates are evaluated and compared to the corresponding experimental quantities. In Section 4, finally, we will briefly discuss the significance of our results.

2. The quark-antiquark potential

It is worthwhile to begin with a short derivation of the running coupling constant (1), in order to establish the domain in which we can trust our theoretical potential. The longitudinal gluon propagator, $iD(q^2)$, can be expanded in terms of the irreducible gluon self-energy or vacuum polarization, $-i\alpha_0 q^2 \Pi(q^2)$, yielding

$$\begin{aligned} iD(q^2) = {} & \frac{-i}{q^2} + \frac{-i}{q^2}(-i\alpha_0 q^2 \Pi(q^2))\frac{-i}{q^2} + \frac{-i}{q^2}(-i\alpha_0 q^2 \Pi(q^2)) \\ & \times \frac{-i}{q^2}(-i\alpha_0 q^2 \Pi(q^2))\frac{-i}{q^2} + \cdots = \frac{-i}{q^2}\frac{1}{1+\alpha_0 \Pi(q^2)}. \end{aligned} \tag{11}$$

Thus, in this approximation, we are led to the straightforward identification of the running coupling 'constant'

$$\alpha(q^2) = \frac{\alpha_0}{1+\alpha_0 \Pi(q^2)}. \tag{12}$$

Here α_0 denotes the 'bare' coupling, i.e. the coupling for which the gluon self-energy vanishes.

The imaginary part of the $\Pi(q^2)$ along the cut on the time-like real axis is related to the gluon decay into gluons and quark-antiquark pairs in the perturbative vacuum of QCD. For massless gluons and quarks we have in first order

$$\operatorname{Im}\Pi(q^2+i\varepsilon)=-B_{Nf}\pi. \tag{13}$$

We now turn to the evaluation of the analytic function $\Pi(q^2)$ via a once subtracted dispersion relation

$$\Pi(q^2)-\Pi(-\mu^2)=-\frac{1}{\pi}\int_0^\infty dM^2\,\operatorname{Im}\Pi(M^2+i\varepsilon)\left[\frac{1}{M^2-q^2}-\frac{1}{M^2+\mu^2}\right] \tag{14}$$

yielding

$$\Pi(q^2)-\Pi(-\mu^2)=B_{Nf}\log(-q^2/\mu^2). \tag{14'}$$

For convenience, the subtraction point has been taken at a space-like momentum transfer, $q^2=-\mu^2$.

Combining equation (12) and (14'), we arrive at

$$\alpha(q^2)=\frac{\alpha(-\mu^2)}{1+\alpha(-\mu^2)B_{Nf}\log(-q^2/\mu^2)} \tag{15}$$

where $\alpha(-\mu^2)$ is the coupling constant, renormalized at $q^2=-\mu^2$. Equation (15) is readily transformed into equation (1) by introducing the scale parameter Λ

$$\Lambda=\mu\exp\left[-\frac{1}{2\alpha(-\mu^2)B_{Nf}}\right]. \tag{16}$$

Thus, the *dressed* gluon propagator (11) develops a branch point at $q^2=0$ where the *bare* propagator has a pole. In addition, the *dressed* propagator has a pole at $q^2=-\Lambda^2$ which represents a 'Landau ghost' [4]) with a positive residue. Thus, in this first order approximation, the gluon can transmute into a massive tachyon. The occurrence of this pole is clearly unphysical and therefore it should be removed. This point will be discussed in greater detail elsewhere [15].

We can trust, however, the discontinuity of $\alpha(q^2)$ across the timelike real axis, since it is related to the physical process of the gluon decay in the perturbative vacuum. With

$$\operatorname{Im}\alpha(q^2+i\varepsilon)=\frac{\pi}{B_{Nf}[(\log q^2/\Lambda^2)^2+\pi^2]}\quad\text{for}\quad q^2>0, \tag{17}$$

one can easily find the spectral representation of $\alpha(q^2)$ in terms of its singularities

$$\alpha(q^2)=B_{Nf}^{-1}\left[\int_0^\infty\frac{dM^2}{[(\log M^2/\Lambda^2)^2+\pi^2](M^2-q^2)}-\frac{\Lambda^2}{q^2+\Lambda^2}\right]. \tag{18}$$

In this form, the contribution along the cut in the complex plane is explicitly separated from the spurious pole term.

We are now ready to perform the Fourier transform (3) based on the spectral representation (18) at spacelike momentum transfers, $q^2=-|\mathbf{q}|^2$. First, we have to

[4]) In the case of QCD it should be called a 'Landau tachyon'.

specify how to integrate around the tachyon pole. The simplest interpretation of the singular integral (3) in terms of a *principal value* leads to a real potential

$$W_0(r) = W_{\text{pole}}(r) + W_{\text{cut}}(r). \tag{19}$$

For $N=3$ and $B_f \equiv B_{Nf}(N=3)$, the contribution of the tachyon pole is

$$W_{\text{pole}}(r) = \frac{4}{3B_f r}(1-\cos \Lambda r), \tag{20}$$

while the cut term is given by

$$W_{\text{cut}}(r) = -\frac{4}{3B_f r}\int_0^\infty \frac{(1-e^{-Mr})\, dM^2}{[(\log M^2/\Lambda^2)^2+\pi^2]M^2}. \tag{21}$$

The potential $W_{\text{cut}}(r)$ is obviously an attractive 'Coulomb like' interaction, represented by the dotted line in Fig. 1 for a particular choice of parameters. The interaction is of varying strength and less singular than the Coulomb potential at

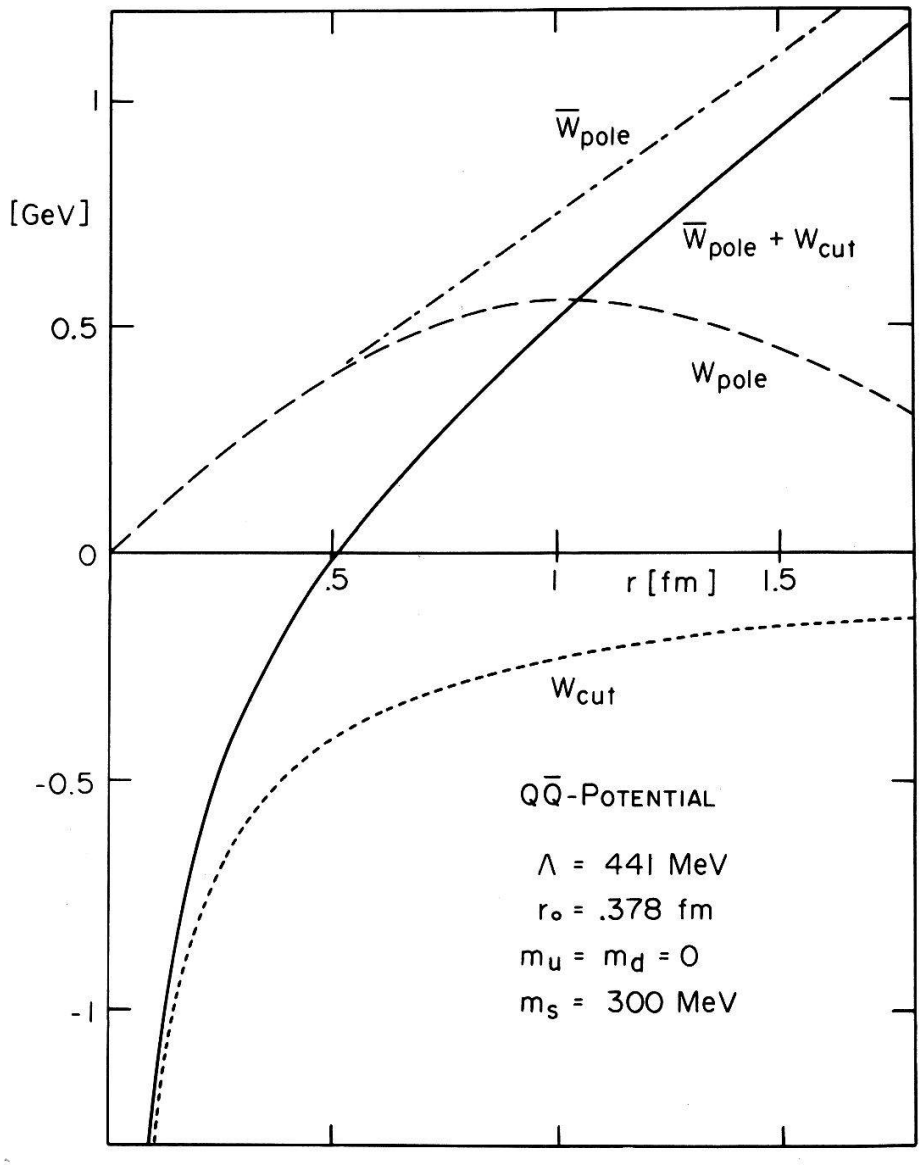

Figure 1
The spin independent quark-antiquark potential.

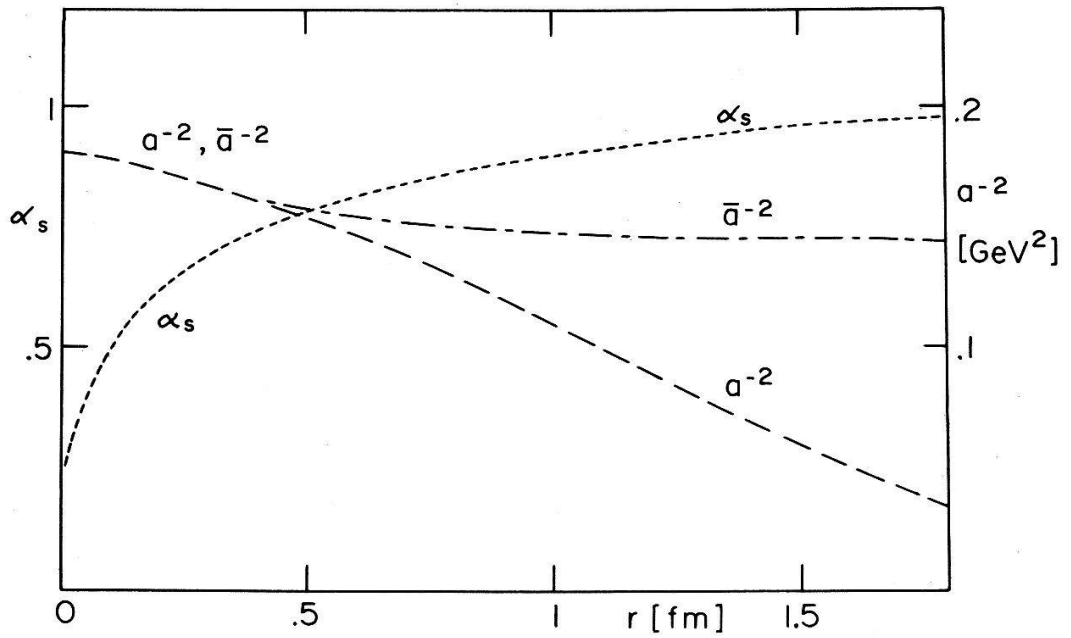

Figure 2
The effective coupling constant $\alpha_s(r)$ and slope parameter $\bar{a}^{-2}(r)$.

short distances. This can be seen in Fig. 2 where the dotted line represents the 'effective coupling constant' defined as

$$\alpha_s(r) = -\tfrac{3}{4} r W_{\text{cut}}(r). \tag{22}$$

It varies between $\alpha_s \approx 0.4$ at $r = 0.05$ fm and $\alpha_s \approx 0.8$ at $r = 0.5$ fm.

The potential $W_{\text{pole}}(r)$, shown for the same set of parameters by the dashed line in Fig. 1, must be taken with more caution. It is tempting to identify this term with a 'confining' potential. However, $W_{\text{pole}}(r)$ cannot describe permanent confinement, since it oscillates and reaches its first maximum of roughly 550 MeV at about 1 fm. While $W_{\text{pole}}(r)$ is probably incorrect for large values of r, there is reason to believe its structure at short distances. Thus, motivated by gauge theories on a lattice [16], we extrapolate $W_{\text{pole}}(r)$ linearly beyond a certain radius r_0

$$\bar{W}_{\text{pole}}(r) = \begin{cases} W_{\text{pole}}(r) & r \le r_0 \\ W_{\text{pole}}(r_0) + W'_{\text{pole}}(r_0)(r - r_0) & r > r_0. \end{cases} \tag{23}$$

The extrapolation radius r_0 is a phenomenological parameter to be determined from the experimental data. The 'linearized' potential $\bar{W}_{\text{pole}}(r)$ is represented by the dashed-dotted line in Fig. 1, while the solid line stands for the total potential,

$$W_0(r) = \bar{W}_{\text{pole}}(r) + W_{\text{cut}}(r), \tag{19'}$$

actually used in the calculation. In order to facilitate the comparison with other models, we have plotted in Fig. 2 the 'effective slope parameters', defined as

$$\bar{a}^{-2}(r) = \bar{W}_{\text{pole}}(r)/r. \tag{24}$$

It varies between $\bar{a}^{-2} = 0.18\,\text{GeV}^2$ for short and $\bar{a}^{-2} = 0.14\,\text{GeV}^2$ for large distances.

As a final point, let us discuss how to include the effect of finite quark masses on the polarizability of the perturbative vacuum. The up and down quarks can be

assumed as massless, but we should allow for a finite mass of the strange and heavier quarks. The gluon part of the irreducible vacuum polarization is for $q^2>0$

$$\operatorname{Im}\Pi_{g\to gg}(q^2+i\varepsilon)=-\tfrac{11}{4}, \tag{25}$$

while each quark flavor ($Q=u, d, s, c, \ldots$) contributes

$$\operatorname{Im}\Pi_{g\to Q\bar{Q}}(q^2+i\varepsilon)=\frac{1}{6}\left(1+\frac{2m_Q^2}{q^2}\right)\sqrt{1-\frac{4m_Q^2}{q^2}} \tag{26}$$

for $q^2>4m_Q^2$ which corresponds to distances $r\lesssim(2m_Q)^{-1}$. We could certainly use equations (12), (14), (25) and (26) to derive the exact form of the potential, but it is sufficient to change the value of f in equation (2) by one unit as r becomes smaller than $(2m_Q)^{-1}$. Thus, if we restrict ourselves to three quark flavors, $m_u=m_d=0$ and $m_s\neq 0$, the constant B_f in equations (20) and (21) is replaced by the function $B_{\text{eff}}(r)$ defined as

$$\frac{1}{B_{\text{eff}}(r)}=\frac{1}{B_2}+\left(\frac{1}{B_3}-\frac{1}{B_2}\right)\exp(-2m_s r) \tag{27}$$

which interpolates smoothly between the two limiting cases

$$\begin{cases}\dfrac{1}{B_{\text{eff}}(r)}\approx\dfrac{1}{B_3} & r\ll(2m_s)^{-1}\\[2ex] \dfrac{1}{B_{\text{eff}}(r)}\approx\dfrac{1}{B_2} & r\gg(2m_s)^{-1}.\end{cases} \tag{28}$$

The exponential range of $B_{\text{eff}}^{-1}(r)$ is adjusted to the approximate range of the vacuum polarization potential arising from strange quark-antiquark pairs.

3. Numerical results

3.1. *The spectra*

We now turn to the discussion of the numerical results. A straightforward potential description of the states above flavor threshold is unreliable due to the strong coupling to the decay channels. Thus, we will restrict ourselves to the study of the low-lying states. The charmonium and bottomium spectra are evaluated solving the Schrödinger equation with the potential shown on Fig. 1. We insert the masses of the light quarks, $m_u=m_d=0$ and $m_s=300$ MeV, from the bag model. For charmonium, the three free parameters of the model, Λ, r_0, and m_c, are determined by fitting the $1S$, $2S$, and $1P$ levels to the experimental $1\,^3S_1$ (3.097), $2\,^3S_1$ (3.686), and to the center of gravity of the $1\,^3P_{0,1,2}$ levels at 3.523 GeV [17], respectively. The fit parameters $\Lambda=441$ MeV, $r_0=0.378$ fm, and $m_c=1.525$ GeV, are compatible with what one may expect from other sources [4, 13]. For the bottomium spectrum we use the same potential. The only parameter left, the bottom quark mass m_b, is adjusted to the experimental $1\,^3S_1$ (9.46) level of bottomium [18] yielding $m_b=4.929$ GeV.

In Fig. 3 and Table 1, we present various quarkonium spectra. The agreement between theory and experiment in the case of charmonium is largely due to

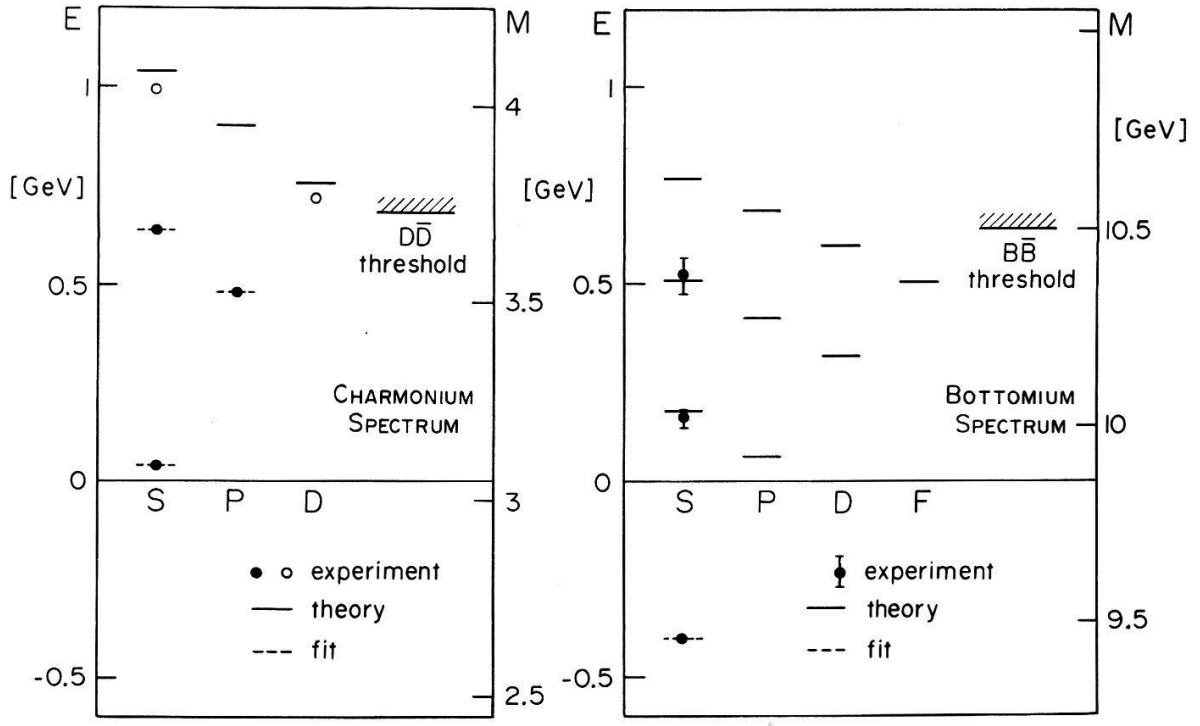

Figure 3
The orthocharmomium and orthobottomium spectra. The observed states are compared to calculations with a spin independent force.

the fact that the three lowest levels have been fitted. Thus, the only independent tests of the model are the experimental $3\,^3S_1$ (4.030) and $1\,^3D_1$ (3.772) levels. Unfortunately, the theoretical prediction of the first is unreliable, since it is far above charm threshold, while the latter cannot be compared to the calculated center of gravity of the $1\,^3D_{1,2,3}$ levels without introducing spin dependent forces.

The real test of our QCD potential is the bottomium spectrum. Here the observed $2\,^3S_1$ (10.02) and $3\,^3S_1$ (10.38) levels are below bottom threshold, and represent therefore a conclusive test of the model. Our calculations agree very well with the observed bottomium spectrum, thus confirming the reliability of the first order QCD potential. In fact, it includes both concepts, asymptotic freedom

Table 1
The orthoquarkonium spectra for $(c\bar{c})$, $(b\bar{b})$, and $(b\bar{c})$ bound states in GeV. The observed states are compared to calculations with a spin independent force (* ≡ fit).

	$(c\bar{c})$		$(b\bar{b})$		$(b\bar{c})$
state	experiment	theory	experiment	theory	theory
4S				10.628	
3S	(4.030±0.010)	4.090	10.38±0.04	10.370	7.30
2S	3.686±0.003	3.686*	10.02±0.02	10.039	6.93
1S	3.097±0.002	3.097*	9.46±0.01	9.460*	6.34
3P				10.543	
2P		3.951		10.275	7.18
1P	3.523±0.005	3.523*		9.921	6.77
2D				10.456	
1D	(3.772±0.006)	3.806		10.176	7.05
1F				10.366	

and linear confinement at large distances, and does therefore a much better job than e.g. the Coulomb+linear potential. We recall here that the original Coulomb+linear potential [4] fails by about 150 MeV in the description of the $2S$ and $3S$ bottomium states. Assuming that the flavor threshold is at 680 MeV, independent of the quark mass, we predict the $1\,^1S_0$ state of the bottom meson $B^- = (b\bar{u})$ at 5.27 GeV. Recently a bottom meson has been reported at 5.3 GeV [19].

We have studied in detail the quark contribution to the vacuum polarization. The major effect on the spectrum arises from the massless up and down quarks. As expected, the quark contribution increases the overall level spacing of the spectrum. The massive strange quark, however, affects mainly the lowlying states, since only the short-range part of the interaction is changed. Thus, it lowers e.g. the masses of the J/ψ and Υ particles by 13 and 38 MeV, respectively. Of course, the charmonium and bottomium data could be reproduced omitting entirely the strange quark vacuum polarization. In fact, we obtain a similar fit to the observed spectra with $\Lambda = 472$ MeV, $r_0 = 0.462$ fm, $m_c = 1.505$ GeV, and $m_b = 4.909$ GeV which sheds some light in the uncertainty of the parameters. In this context, it is interesting to note that the mass difference, $m_b - m_c = 3.404$ GeV, is to a large extent independent of the choice of the potential parameters [20].

The quarkonium spectrum, plotted as a function of the quark mass m_Q, is shown in Figs. 4 and 5. While the excitation energy to the first excited state remains roughly constant ($\approx$600 MeV) in the range of $1.5\text{ GeV} \lesssim m_Q \lesssim 9\text{ GeV}$, it increases rapidly at larger quark masses. For example at $m_Q = 15$ GeV we have already $M(2\,^3S_1) - M(1\,^3S_1) = 707$ MeV. Here the $1S$-wave function is concentrated in a domain of roughly 0.1 fm which makes the excitation energy very sensitive to the short-range behavior of the potential and thus to the vacuum polarization contribution of the heavy quarks.

Of course, the energy levels of other nonrelativistic quark-antiquark bound states like the $(b\bar{c})$, $(t\bar{c})$, and $(t\bar{b})$ systems can be calculated, as well. Introducing the reduced and the total mass of the $(b\bar{c})$-system, i.e.

$$m_{bc} = \frac{m_b m_c}{m_b + m_c} \tag{29}$$

and

$$M = m_b + m_c + E(2m_{bc}) \tag{30}$$

we can predict from Figs. 4 and 5 the triplet states of the $(b\bar{c})$-mesons (Table 1).

3.2. *Spin structure*

It is worthwhile to begin with a brief discussion of the current data on the spin dependent interaction. The spin orbit and tensor splittings of the P-levels in charmonium are well established. Based on first order perturbation theory and equation (6) we obtain

$$\begin{cases} M(1\,^3P_2) = M(1\,^3P) + W_1(1P) - \frac{2}{3}W_2(1P) \\ M(1\,^3P_1) = M(1\,^3P) - W_1(1P) + 2W_2(1P) \\ M(1\,^3P_0) = M(1\,^3P) - 2W_1(1P) - 4W_2(1P) \end{cases} \tag{31}$$

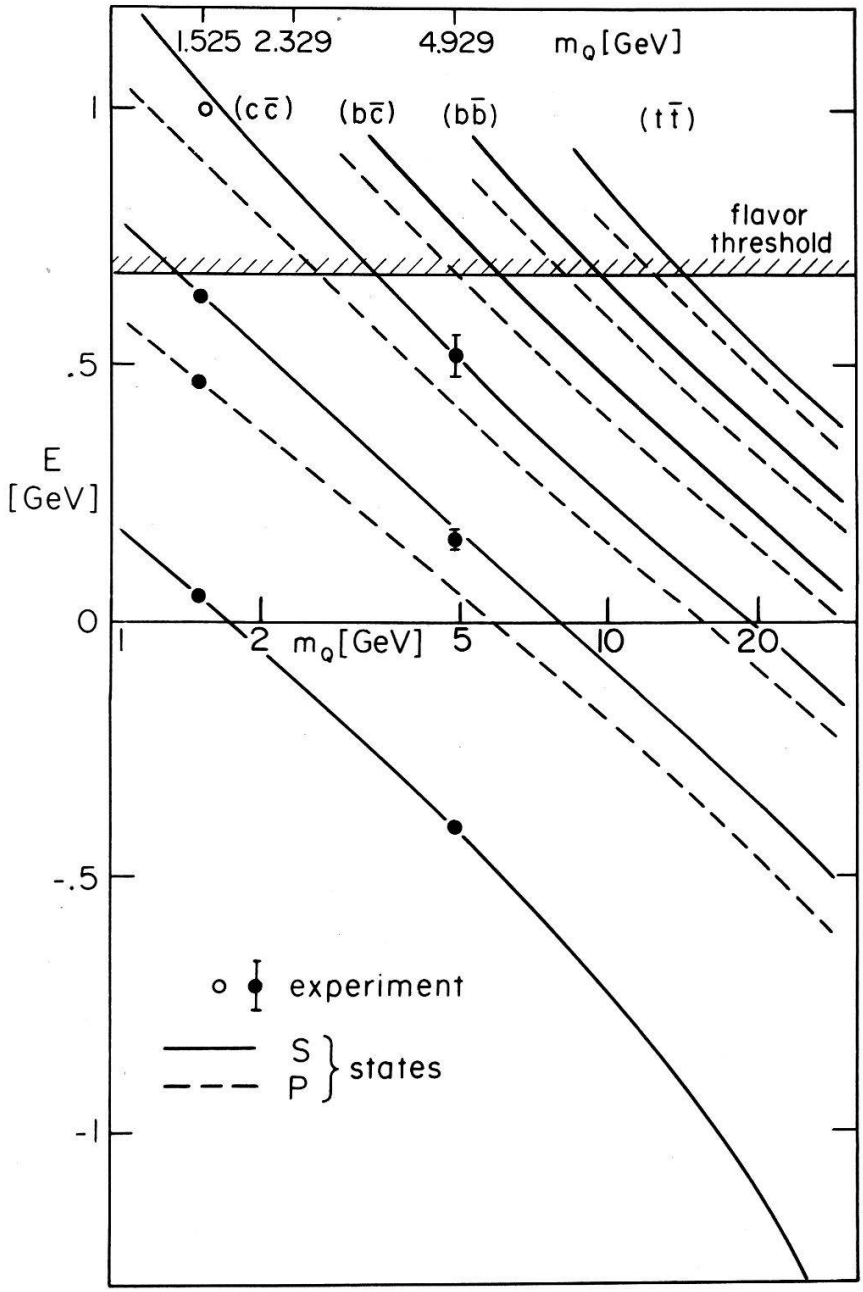

Figure 4
The energy levels of the S and P states of quarkonium as a function of the quark mass m_Q.

From the experimental P-levels $1\,^3P_2$ (3.554), $1\,^3P_1$ (3.508), and $1\,^3P_0$ (3.413) [17] one can deduce the center of gravity of the $1\,^3P_{0,1,2}$ states (Table 1)

$$M(1\,^3P) = 3.523\ \text{GeV} \tag{32}$$

and the expectation values of the spin-orbit and tensor interaction (Table 2)

$$\begin{cases} W_1^{\text{exp}}(1\,P) = 35\ \text{MeV} \\ W_2^{\text{exp}}(1\,P) = 10\ \text{MeV}. \end{cases} \tag{33}$$

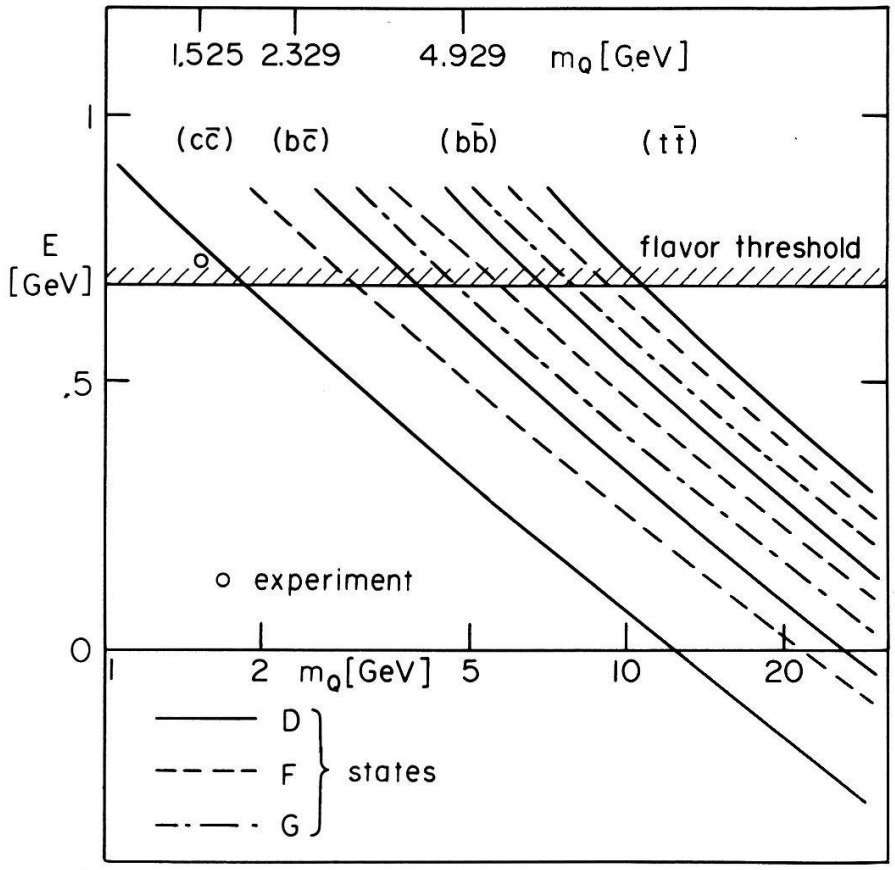

Figure 5
The energy levels of the D, F, and G states of quarkonium as a function of the quark mass m_Q.

Table 2
The observed and theoretical expectation values of the spin-dependent interaction in MeV. The theoretical numbers for charmonium and bottomium are calculated using a pure vector potential.

	$(c\bar{c})$						$(b\bar{b})$		
	experiment			theory			theory		
state	W_1	W_2	W_3	W_1	W_2	W_3	W_1	W_2	W_3
$4S$							0	0	3.0
$3S$	0	0		0	0	15.4	0	0	3.8
$2S$	0	0		0	0	20.0	0	0	5.4
$1S$	0	0	30.3?	0	0	36.6	0	0	13.4
$3P$							13.9	1.7	1.2
$2P$				59.3	6.5	6.8	16.9	2.1	1.4
$1P$	35	10		76.1	8.2	8.9	24.4	3.1	2.0
$2D$							7.3	0.8	0.8
$1D$	$W1+\frac{2}{3}W_2$ = 11.3?			37.1	3.4	5.6	8.9	1.0	1.0
$1F$							5.2	0.5	0.7

Similarly, we have for the D-states in first order

$$\begin{cases} M(1\,^3D_3) = M(1\,^3D) + 2W_1(1\,D) - \frac{4}{7}W_2(1\,D) \\ M(1\,^3D_2) = M(1\,^3D) - W_1(1\,D) + 2W_2(1\,D) \\ M(1\,^3D_1) = M(1\,^3D) - 3W_1(1\,D) - 2W_2(1\,D) \end{cases} \tag{34}$$

from the observed $1\,^3D_1$ (3.772) level and the theoretical estimate for the center of gravity of the $1\,^3D_{1,2,3}$-states, $M(1\,^3D) = 3.806$ GeV, we conclude (Table 2)

$$W_1^{\exp}(1\,D) + \tfrac{2}{3}W_2^{\exp}(1\,D) = 11.3\ \text{MeV}(?). \tag{35}$$

This relation, however, is less reliable, since it depends also on the theoretical value of $M(1\,^3D)$.

The hyperfine splitting of the various states is given in first order by

$$M(n^3L) - M(n^1L) = 4W_3(nL) \qquad L = S, P, \ldots; n = 1, 2, \ldots \tag{36}$$

Here the experimental situation is less clear. In fact, since the states at 2.830, 3.454, and 3.590 GeV have not been confirmed by more refined experiments at SLAC [19], no paracharmonium state is really well established. However, recently a candidate has been reported at 2.976 GeV [19] which might very well represent the long expected η_c, the $1\,^1S_0$ partner of the J/ψ particle, yielding (Table 2)

$$W_3^{\exp}(1\,S) = 30.3\ \text{MeV}(?). \tag{37}$$

Our calculated matrix elements are shown in Table 2 for charmonium and bottomium. Here the spin independent potential W_0 is assumed to be of vector type. For charmonium, the tensor splitting $W_2(1\,P) = 8.2$ MeV and the hyperfine splitting $W_3(1\,S) = 36.6$ MeV agree reasonably well with the experimental values of $W_2^{\exp}(1\,P) = 10$ MeV and $W_3^{\exp}(1\,S) = 30.3$ MeV(?), respectively. However, the theoretical spinorbit splitting $W_1(1\,P) = 76.1$ MeV is about a factor two larger than the experimental value of $W_1^{\exp}(1\,\text{P}) = 35$ MeV. The discrepancy is even larger for the $1\,D$-states, since, instead of 11.3 MeV (equation 35), our model predicts

$$W_1(1\,D) + \tfrac{2}{3}W_2(1\,D) = 39.2\ \text{MeV}. \tag{38}$$

Thus, even if our estimate of $M(1\,^3D)$ was too low about 30 MeV, the theoretical prediction (38) is still about twice as large as the experimental one. This may indicate the presence of an additional scalar potential $S_0(r)$. We will return to this point below.

Using the matrix elements given in Table 2 and equations (31) and (34), we can deduce the energy levels of the $1\,P$ and $1\,D$ states in orthobottomium

$$M(1\,^3P_{0,1,2}) = (9.860, 9.903, 9.944)\ \text{GeV} \tag{39}$$

$$M(1\,^3D_{1,2,3}) = (10.147, 10.169, 10.193)\ \text{GeV}. \tag{40}$$

However, as in the case of charmonium, we should not trust this prediction too much, except for the fact that the splittings are much smaller than for charmonium.

In spite of the numerous attempts to understand the observed splittings of the charmonium states quantitatively, the spin structure of the quark-antiquark

interaction is still an open question. Following the conventional approach within the framework of the generalized Breit-Fermi interaction (10) one may introduce a scalar component $S_0(r)$ in the spin independent potential (9). The one-gluon-exchange potential has presumably vector character at short distances. But at intermediate and large distances, when the confining mechanism sets in, the potential may acquire an unknown scalar component $S_0(r)$. Since there is experimental information on the splittings of three states ($1S$, $1P$, and $1D$) which probe different space regions, one may parameterize the shape of the scalar potential, however, at the expense of the predicting power of the theory. With a simple power law ansatz

$$S_0(r) = \begin{cases} Ar^n & r \leq r_1 \\ Ar_1^n & r > r_1 \end{cases} \tag{41}$$

and $V_0(r) = W_0(r) - S_0(r)$, the scalar contribution to the various spin dependent potentials is

$$\begin{cases} \delta W_1(r) = -\dfrac{2nAr^{n-2}}{m_Q^2} \\ \delta W_2(r) = -\dfrac{(2-n)nAr^{n-2}}{12m_Q^2} \quad \text{for} \quad r \leq r_1 \\ \delta W_3(r) = -\dfrac{n(n+1)Ar^{n-2}}{6m_Q^2} \end{cases} \tag{42}$$

and $\delta W_1(r) = \delta W_2(r) = \delta W_3(r) = 0$ for $r > r_1$. A good fit to the observed spin dependence is obtained with

$$\begin{cases} n = 3 \\ A = 0.961 \text{ GeV/fm}^3 \\ r_1 = 0.805 \text{ fm}. \end{cases} \tag{43}$$

3.3. *Leptonic decays and electromagnetic transitions*

An interesting consistency check of the model are the leptonic decay widths usually calculated through the van Royen-Weisskopf [21] formula

$$\Gamma(n\,^3S_1 \to l^+l^-) = \frac{16\pi^2\alpha^2}{M(n\,^3S_1)^2} |\psi_n(0)|^2 e_Q^2. \tag{44}$$

Here α denotes the fine structure constant, e_Q is the charge of the quark in units of e, and $\psi_n(0)$ is the $n\,^3S_1$-state wave function at the origin. This equation, however, is subject to large radiative corrections, arising from the exchange of gluons, which tend to suppress the leptonic widths dramatically. In fact, equation (44) should read

$$\Gamma(n\,^3S_1 \to l^+l^-) = \frac{16\pi^2\alpha^2}{M(n\,^3S_1)^2} |\psi_n(0)|^2\, e_Q^2 F(m_Q^2). \tag{45}$$

The correction factor $F(m_Q^2)$ has been evaluated to first order in $\alpha(q^2)$ [22] giving

$$F(m_Q^2)=1-\frac{4}{3}\frac{4}{\pi}\alpha(m_Q^2) \tag{46}$$

where $\alpha(m_Q^2)$ denotes the strong coupling constant at timelike momentum transfers. Since the correction is rather large, one may conclude that the first order result is unreliable. Thus, at the present stage, $F(m_Q^2)$ is best kept as a free parameter to be determined from the charmonium and bottomium data. In Table 3 the leptonic decay widths are shown for charmonium and bottomium. Here the theoretical widths of the ground states have been fitted to their experimental values by introducing the scale factors

$$F(m_c^2)=0.55 \quad \text{and} \quad F(m_b^2)=0.62. \tag{47}$$

In first order, these correspond to the coupling constants of

$$\alpha(m_c^2)=0.27 \quad \text{and} \quad \alpha(m_b^2)=0.23, \tag{48}$$

respectively, which are somewhat larger than expected from the three gluon decays. Thus, only the widths of the excited states are meaningful in our comparison of the theoretical and experimental data in Table 3. The widths of the $2S$ states agree very nicely with the experimental data.

For completeness, we also mention the electromagnetic transition rates for charmonium. In nonrelativistic approximation, the rates for electric dipole transitions are given by [14]

$$\begin{aligned}\Gamma(E1, 2\,^3S_1 \to 1\,^3P_J)&=\tfrac{4}{27}(2J+1)e_Q^2\alpha[M(2\,^3S_1)-M(1\,^3P_J)]^3\langle 1P|\,r\,|2S\rangle^2\\ \Gamma(E1, 1\,^3P_J \to 1\,^3S_1)&=\tfrac{4}{9}e_Q^2\alpha[M(1\,^3P_J)-M(1\,^3S_1)]^3\langle 1S|\,r\,|1P\rangle^2\end{aligned} \tag{49}$$

where $\langle n'L'|\,r\,|nL\rangle$ is the electric dipole matrix element

$$\langle n'L'|\,r\,|nL\rangle=\int_0^\infty U_{n'L'}(r)rU_{nL}(r)r^2\,dr, \tag{50}$$

and $U_{nL}(r)$ the normalized radial wave function. Using the experimental masses of the $1\,^3S_1$, $2\,^3S_1$, and $1\,^3P_{0,1,2}$ states, the $2S-1P$ transition rates

$$\Gamma(E1, 2\,^3S_1 \to 1\,^3P_{0,1,2})=(70, 58, 40)\ \text{keV} \tag{51}$$

are a factor 2 or 3 larger than the observed $E1$ transition rates of (17 ± 8) keV.

Table 3
The experimental and theoretical leptonic widths in keV for charmonium and bottomium. The theoretical values are computed with $F(m_c^2)=0.55$ and $F(m_b^2)=0.62$ (* ≡ fit).

	$(c\bar{c})$		$(b\bar{b})$	
state	experiment	theory	experiment	theory
$4S$				0.23
$3S$	(0.75 ± 0.15)	1.3		0.30
$2S$	2.10 ± 0.30	2.0	0.33 ± 0.10	0.45
$1S$	4.80 ± 0.60	4.8*	1.20 ± 0.20	1.2*

This discrepancy indicates the limits of our present understanding of the short-range quark-antiquark interaction. Clearly more work is needed on higher order QCD corrections to the electromagnetic transition rates. For the $1P-1S$ transition rates we obtain

$$\Gamma(E1, 1\,^3P_{0,1,2} \to 1\,^3S_1) = (194, 428, 583)\ \text{keV}. \tag{52}$$

We now turn to the magnetic dipole transitions in charmonium. The description of the forbidden transitions is uncertain due to coherent relativistic effects. We therefore focus on the allowed magnetic transitions [14]

$$\Gamma(M1, n\,^3S_1 \to n\,^1S_0) = \frac{4}{3}\frac{e_Q^2}{m_Q^2}\alpha[M(n\,^3S_1 - M(n\,^1S_0)]^3. \tag{53}$$

Assuming that the $1\,^1S_0$ state is at 2.951 GeV as predicted by our model, we obtain

$$\Gamma(M1, 1\,^3S_1 \to 1\,^1S_0) = 5.8\ \text{keV}. \tag{54}$$

However, using the reported $1\,^1S_0$ candidate at 2.976 GeV [19], the decay width for a magnetic dipole transition

$$\Gamma(M1, 1\,^3S_1 \to 1\,^1S_0) = 3.3\ \text{keV} \tag{55}$$

is much closer to the experimental upper limit of 1.1 keV for the transition. Placing the $2\,^1S_0$ state at 3.606 GeV, our model predicts a $2S$-transition rate of

$$\Gamma(M1, 2\,^3S_1 \to 2\,^1S_0) = 1\ \text{keV} \tag{56}$$

which is not in contradiction with the experiment.

4. Conclusions

We have described nonrelativistic heavy quark-antiquark bound states in the framework of quantum chromodynamics. The static quark-antiquark potential is

$$W_0(r) = -\frac{4}{3}\frac{\alpha_s(r)}{r} + \bar{a}^{-2}(r)r \tag{57}$$

where both the 'effective' coupling constant $\alpha_S(r)$ and the slope parameter $\bar{a}^{-2}(r)$, vary significantly (Fig. 2) in the region of interest.

Our calculations reproduce the observed orthocharmonium and orthobottomium spectra quite well. The agreement between the theory and the experiment not only confirms the validity of the perturbative approach to QCD and asymptotic freedom, but also establishes a strict quantitative relation between the parameters of the theory and experiment. We obtain a scale parameter of $\Lambda = 441$ MeV, consistent with estimates from deep inelastic reactions [13]. The quark masses, $m_c = 1.525$ and $m_b = 4.929$ GeV, as well as the phenomenological extrapolation radius $r_0 = 0.378$ fm seem reasonable.

For a general $SU(N)_{\text{color}} \otimes SU(f)_{\text{flavor}}$ theory of strong interactions the 'effective' strength of the quark-antiquark interaction in a color singlet state is given by

the ratio (see equations (2) and (3'))

$$\frac{C_N}{B_{Nf}} = \frac{6\pi}{11} \frac{1-1/N^2}{1-2f/11N}. \tag{58}$$

Thus, for reasonable values of N and f, this expression is rather insensitive to the number of colors and flavors. While the fit parameters Λ, r_0, m_c and m_b will slightly vary if we change the flavor (or color) content of the theory, the mass difference, $m_b - m_c = 3.404\,\text{GeV}$, is remarkably stable. Moreover, the fit to the observed spectra remains equally good. It seems therefore difficult to draw any definite conclusion concerning the number of colors and flavors which are required to describe the experimental spectra adequately. However, our calculations are consistent with three colors and three flavors: two massless up and down quarks, $m_u = m_d = 0$, and a massive strange quark of $m_s = 300\,\text{MeV}$. In view of the theoretical and experimental uncertainties, the electromagnetic transition rates and the leptonic decay widths are in reasonable agreement with the experimental data. However, the detailed spin structure of the quark-antiquark interaction, in particular the Lorentz character of the potential $W_0(r)$, still remains to be understood. In this context, it is interesting to note that the introduction of a scalar potential of the type $S_0(r) \sim r^3$ which may describe the transition from the perturbative to the real QCD vacuum helps improve the spin splittings significantly.

Concluding we would like to emphasize that, if the top quark exists, the toponium spectrum will be crucial test for the model. Assuming a top quark mass of $m_t \gtrsim 20\,\text{GeV}$, toponium will probe much more the domain that can be described by perturbative QCD and that is presumably less sensitive to phenomenological modifications at large distances.

References

[1] T. Appelquist and H. D. Politzer, Phys. Rev. Letters *34* (1975) 43; Phys. Rev. *D12* (1975) 1404; A. DeRújula and S. L. Glashow, Phys. Rev. Lett. *34* (1975) 46; T. Appelquist *et al.*, Phys. Rev. Letters *34* (1975) 365.

[2] See e.g.: Y. Hara, Rapporteur talk XIX Int. Conf. on High Energy Physics, Tokyo, August 1978.

[3] See e.g.: W. Bardeen, H. Fritzsch, and M. Gell-Mann, in *Scale and Conformal Symmetry and Hadron Physics* (ed. R. Gatto, New York, 1973).

[4] E. Eichten *et al.*, Phys. Rev. Letters *34* (1975) 369; E. Eichten and K. Gottfried, Phys. Letters *66B* (1977) 286.

[5] C. Quigg and J. L. Rosner, Phys. Letters *71B* (1977) 153; *72B* (1978) 462.

[6] B. Margolis, R. Roskies, and N. DeTakacsy, "*Potential Models for Heavy Quarks and Asymptotic Freedom*". Preprint McGill University, 1978.

[7] W. Celmaster, H. Georgi and M. Machacek, Phys. Rev. *D17* (1978) 879; *17* (1978) 886; W. Celmaster and F. Henyey, Phys. Rev. *D18* (1978) 1688.

[8] G. Bhanot and S. Rudaz, Phys. Letters *78B* (1978) 119.

[9] J. L. Richardson, Phys. Letters *82B* (1979) 272.

[10] J. Rafelski and R. D. Viollier, CERN preprint TH2673 (1979); R. D. Viollier and J. Rafelski, M.I.T. preprint CTP 791 (1979).

[11] J. M. Richard and D. P. Sidhu, Phys. Letters *83B* (1979) 362.

[12] H. D. Politzer, Phys. Rev. Letters *30* (1973) 1346; D. J. Gross and F. Wilczek, Phys. Rev. *D8* (1973) 3633; Phys. Rev. Letters *30* (1973) 1434.

[13] See e.g.: O. Nachtmann, *Proc. of the Int. Symp. on Photon and Lepton Physics*, Hamburg,

August 1977; A. De Rújula, H. Georgi, and H. D. Politzer, Ann. Phys. (N.Y.) *103* (1977) 315; J. G. H. De Groot *et al.*, Phys. Letters *82B* (1979) 292, 456.
[14] See e.g.: J. D. Jackson, *Proc. 1976 Summer Institute on Particle Physics*, SLAC Report No. 198 (1976) p. 147.
[15] J. Rafelski and R. D. Viollier, in preparation.
[16] J. Kogut and L. Susskind, Phys. Rev. *D9* (1974) 3501; *D11* (1975) 395; K. Wilson, Phys. Rev. *D10* (1974) 2445.
[17] N. Barash-Schmidt *et al.*, Phys. Letters *75B* (1978). R. Brandelik *et al.*, Phys. Letters *76B* (1978) 361. P. A. Rapidis *et al.*, Phys. Rev. Letters *39* (1977) 526; *39* (1977) 974E.
[18] C. Berger *et al.*, Phys. Letters *76B* (1978) 243, Z. Physik *C1* (1979) 343; C. W. Darden *et al.*, Phys. Letters *76B* (1978) 246, Phys. Letters *80B* (1979) 419; S. W. Herb *et al.*, Phys. Rev. Letters *39* (1977) 252; W. R. Innis *et al.*, Phys. Rev. Letters *39* (1977) 1240; J. Bienlein *et al.*, Phys. Letters *78B* (1978) 360; K. Ueno *et al.*, Phys. Rev. Letters *42* (1979) 486.
[19] E. Bloom, *Invited talk Int. Symposium on Lepton and Photon Interactions at High Energies*, Batavia, IL, August 1979.
[20] A. Martin, CERN preprint TH 2741.
[21] R. van Royen and V. F. Weisskopf, Nuovo Cimento *50A* (1967) 617.
[22] R. Barbieri *et al.*, Nucl. Phys. *B105* (1976) 125.